

Strong nodeless pairing on separate electron Fermi surface sheets in (Tl, K)Fe_{1.78}Se₂ probed by ARPES

X.-P. Wang,¹ T. Qian,¹ P. Richard,¹ P. Zhang,¹ J. Dong,¹ H.-D. Wang,² C.-H. Dong,² M.-H. Fang,² and H. Ding^{1,*}

¹*Beijing National Laboratory for Condensed Matter Physics,
and Institute of Physics, Chinese Academy of Sciences, Beijing 100190, China*

²*Department of Physics, Zhejiang University, Hangzhou 310027, China*

(Dated: April 24, 2022)

We performed a high-resolution angle-resolved photoemission spectroscopy study of the Tl_{0.63}K_{0.37}Fe_{1.78}Se₂ superconductor ($T_c = 29$ K). We show the existence of two electronlike bands at the M($\pi, 0$) point which cross the Fermi level at similar Fermi wave vectors to form nearly circular electronlike Fermi surface pockets. We observe a nearly isotropic ~ 8.5 meV superconducting gap ($\Delta/k_B T_c \sim 7$) on these Fermi surfaces. Our analysis of the band structure around the Brillouin zone centre reveals two additional electronlike Fermi surfaces: a very small one and a larger one with k_F comparable to the FS pockets at M. Interestingly, a SC gap with a magnitude of ~ 8 meV also develops along the latter FS. Our observations are consistent with the *s*-wave strong coupling scenario.

PACS numbers: 74.25.Jb, 74.70.Xa, 79.60.-i

The amplitude and symmetry of the superconducting (SC) gap of a material are determined by its band structure, its Fermi surface (FS) topology and the pairing mechanism itself. The experimental observation of enhanced gap amplitude on holelike and electronlike FS pockets quasi-nested by the antiferromagnetic (AF) wave vector in iron-based superconductors [1–5] has been widely considered as suggestive of the importance of AF interband scattering in these materials. In particular, the quasi-nesting model is consistent with the strong suppression of superconductivity in heavily hole-doped [6] and heavily electron-doped [7] BaFe₂As₂ compounds, for which the FS quasi-nesting conditions vanish. Recently, this model faced a serious challenge with the discovery of superconductivity above 30 K in heavily electron-doped K_{0.8}Fe_{2-x}Se₂ and (Tl,K)Fe_{2-x}Se₂ [8, 9]. Indeed, previous angle-resolved photoemission spectroscopy (ARPES) measurements revealed only electronlike FS pockets [10, 11].

In this letter, we report high-energy resolution ARPES measurements on the Tl_{0.63}K_{0.37}Fe_{1.78}Se₂ superconductor ($T_c = 29$ K). We observed two electronlike M($\pi, 0$)-centred FS pockets that develop a nearly isotropic SC gap below T_c with a magnitude of ~ 8.5 meV, leading to a $2\Delta/k_B T_c$ of ~ 7 . In addition, a weak electronlike FS pocket with a similar size and a tiny electronlike pocket are also observed at the $\Gamma(0, 0)$ point. The former one also exhibits a SC gap size of about 8 meV. In addition, a high-energy (~ 0.8 eV) incoherent peak undergoes a significant energy shift of ~ 100 meV through the metal-nonmetal crossover around 70K, while the low-energy valence band shows little change. We discuss the possible implications of the SC gap symmetry and the FS topology for the SC pairing mechanism in this unusual iron-

based superconductor .

Single crystals of Tl_{0.63}K_{0.37}Fe_{1.78}Se₂ ($T_c^{\text{onset}} = 29.1$ K; $T_c^{\text{mid}} = 28.6$ K; $T_c^{\text{zero}} = 27.5$ K) were grown by the Bridgeman method [9]. The precise composition was determined using an Energy Dispersive X-ray Spectrometer (EDXS). The lattice parameters $a = 3.85$ Å and $c = 14.05$ Å were obtained by fitting XRD data. We performed ARPES measurements at the Institute of Physics, Chinese Academy of Sciences using the He I α resonance line ($h\nu = 21.218$ eV). The angular resolution was set to 0.2° while the energy resolution was set to 4-7 meV for high-resolution measurements. Samples with a typical size of $\sim 2 \times 2$ mm² were cleaved *in situ* and measured between 10 and 35 K in a working vacuum better than 5×10^{-11} . The Fermi energy (E_F) of the samples was referenced to that of a gold film evaporated onto the sample holder. For convenience, we describe all the results using the 1 Fe site/unit (or unfolded) cell notation.

In Fig. 1(a), we show a momentum-resolved photoemission intensity mapping of Tl_{0.63}K_{0.37}Fe_{1.78}Se₂ recorded in the normal state (35 K) and integrated over a 10 meV window centred at the Fermi level (E_F). As with other A_xFe₂Se₂ materials with similar T_c values [10, 11], the dominant feature of the mapping is an almost circular electronlike FS pocket centred at the M point. We note that the intensity patterns around M1($\pi, 0$) and M2(0, π) are different due to different matrix elements resulting from different $\mathbf{A} \cdot \mathbf{p}$ configurations, where \mathbf{A} is the potential vector associated with the incoming light. In order to extract the SC gap size precisely along the FS and to investigate its symmetry, we performed high-resolution measurements along cuts crossing the Fermi surface. In Fig. 1(b), we display a series of energy distribution curves (EDCs) along cut1 given in Fig. 1(a). The EDCs show a peak dispersing towards E_F that starts bending back at the Fermi wave vector (k_F), a hallmark of Bogoliubov dispersion in the SC state. By comparing SC-state and normal-state EDCs measured at the same k_F , as shown

*Electronic address: dingh@iphy.ac.cn

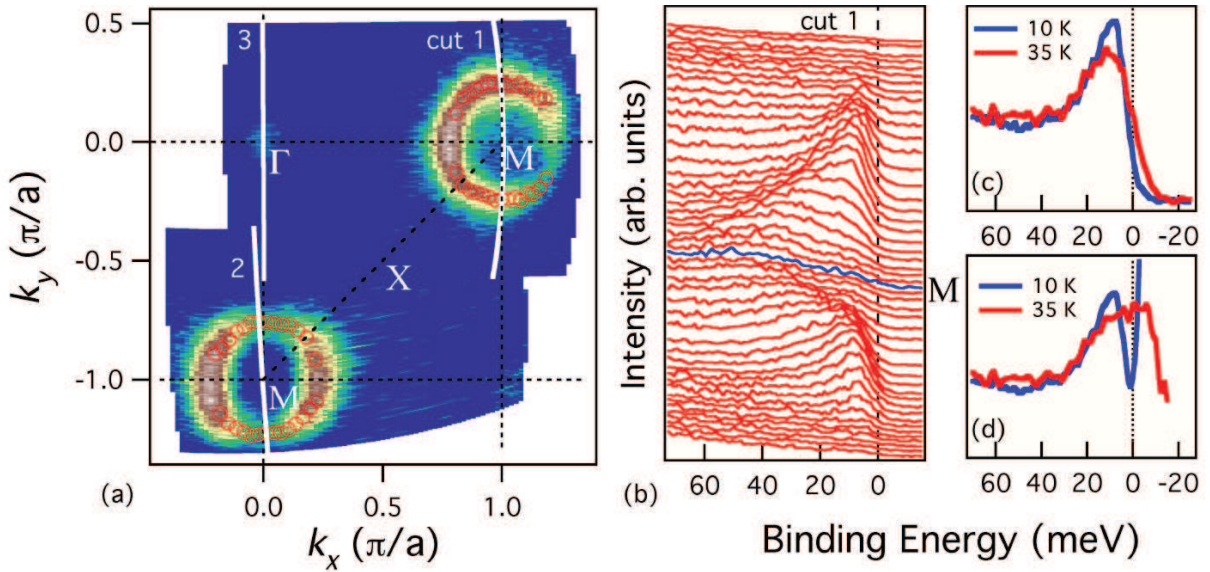


FIG. 1: (Colour on-line) (a) Momentum-resolved photoemission intensity mapping of $\text{Tl}_{0.63}\text{K}_{0.37}\text{Fe}_{1.78}\text{Se}_2$ recorded in the normal state (35 K) and integrated over a 10 meV window centred at E_F . The small red circles indicate the FS obtained from the momentum distribution curve (MDC) peak position at E_F . (b) EDCs recorded along cut1 from panel (a). The blue line indicate the spectrum at the M point. (c) EDC at k_F recorded at 10 and 35 K. (d) Same as (c) but after division by the Fermi-Dirac function.

in Fig. 1(c), one sees that the leading edge of the SC-state EDC shifts away from E_F . After the Fermi-Dirac function is divided out from the spectra [Fig. 1(d)], the normal-state EDC exhibits a peak at E_F , while the SC-state EDC remains gapped.

The raw energy distribution curves (EDCs) at k_F are given in Fig. 2(a). Following a standard procedure in ARPES, we take advantage of the particle-hole symmetry at k_F by symmetrizing the spectra to approximately remove the Fermi-Dirac function. The symmetrized EDCs are shown in Fig. 2(b). The SC gap size Δ is approximated by half the distance between the two peaks. Obviously, the peak position does not vary much with momentum within experimental uncertainties. We report the gap size extracted for different samples mounted with different orientations in Fig. 2(c). We find that the SC gap size averages at ~ 8.5 meV with little room for anisotropy and even less for nodes, at least at the particular k_z value corresponding to $h\nu = 21.218$ eV, in agreement with a previous report on $\text{A}_x\text{Fe}_2\text{Se}_2$ ($A = \text{K}, \text{Cs}$) [10]. This gap size leads to a $2\Delta/k_B T_c$ ratio of ~ 7 , indicating that the SC pairing in this material is in the strong coupling regime. The temperature dependence of spectra recorded at a single k_F point are displayed in Fig. 2(d), and the corresponding symmetrized EDCs are shown in Fig. 2(e). Interestingly, the temperature (T) dependence of the SC gap given in Fig. 2(d) indicates that the SC gap size may not close with temperature increasing, but rather fill in gradually up to T_c . Such behaviour has been reported recently in $\text{NaFe}_{0.95}\text{Co}_{0.05}\text{As}$ [12].

The FS pockets at the M point encloses an area corresponding to 4.5 % of the Brillouin zone (1 Fe site/unit

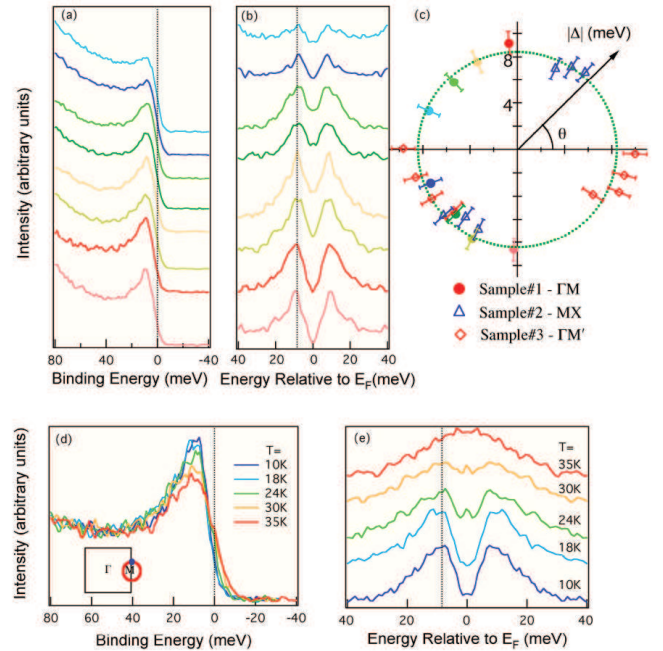


FIG. 2: (Colour on-line) (a) Spectra recorded in the SC state (10 K) at different location around the M-centred electron like FS. The colour of the spectra correspond to their angular locations, which are given in panel (c) (sample 1; plain symbols). (b) Corresponding symmetrized EDCs. (c) Polar distribution of the SC gap size along the FS for 3 different samples. (d) Temperature dependence of EDC spectra at k_F . The inset show the momentum location of the EDC. (e) Corresponding symmetrized EDCs.

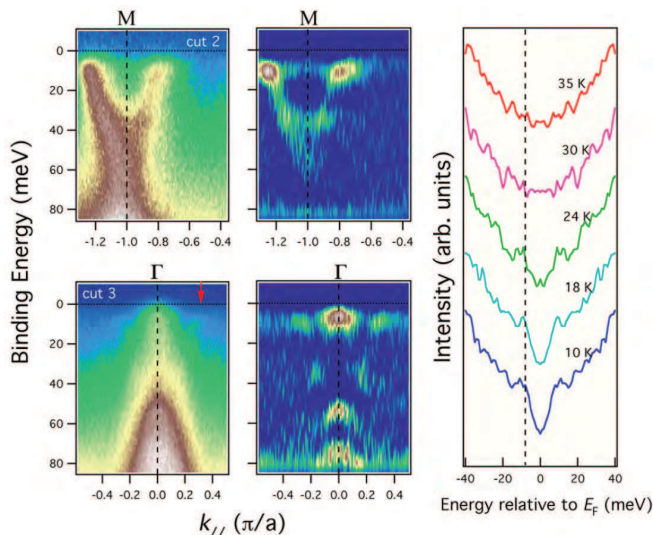


FIG. 3: (Colour on-line) (a) ARPES intensity plot along a cut passing through the M point [cut2 from Fig. 1(a)]. (b) Corresponding energy-second derivative intensity plot. (c) ARPES intensity plot along a cut passing through the Γ point [cut3 from Fig. 1(a)]. (d) Corresponding energy-second derivative intensity plot. (e) Temperature evolution of the symmetrized EDCs at the k_F position indicated by an arrow in (c).

cell description). This leads to a much smaller electron doping than expected from the Luttinger theorem. However, previous ARPES measurements on other iron-based superconductors indicate that there are two electronlike FS pockets with similar k_F 's centred at the M point [1, 3, 4, 7, 12]. To confirm that this observation holds for $\text{Tl}_{0.63}\text{K}_{0.37}\text{Fe}_{1.78}\text{Se}_2$, we display the ARPES intensity plot along cut2 [see Fig. 1(a)] in Fig. 3(a), and the corresponding energy-second derivative intensity plot in Fig. 3(b). The data suggest that there are two distinct bands with bottoms around 40 and 60 meV, respectively. Within our experimental resolution, the bands have approximately the same k_F values.

The approximate 2-fold degeneracy of the electronlike FS pocket at M leads to an electron counting of 18% electron per Fe, which is still not enough to afford for the 31.5% electron per Fe expected from the Luttinger theorem for this material. We now turn our attention to the band structure around the Γ point. Fig. 3(c) and Fig. 3(d) give the ARPES intensity plot along cut3 [see Fig. 1(a)] and the corresponding second derivative intensity plot along energy, respectively. The strongest feature is a holelike band topping around 50 meV below E_F . We also found a tiny electronlike feature with a bottom around 10 meV below E_F that has been reported previously in $\text{A}_x\text{Fe}_2\text{Se}_2$ ($A = \text{K}, \text{Cs}$) [10]. In addition, we observe a large electronlike band at Γ with a k_F similar to that of the electron bands at M. The inclusion of the electronlike bands at the Γ point raises the electron counting to 32% electrons per Fe, which is in reasonable agreement with the nominal composition. As shown in Fig. 3 (e), where

the EDC spectra at k_F are presented as a function of temperature, a SC gap that vanishes above T_c is found along the large electronlike FS at Γ . Interestingly, the SC gap size (~ 8 meV) is almost the same as the one we find at the M point.

Another major difference we observed in $\text{K}_{0.8}\text{Fe}_{1.7}\text{Se}_2$ from other iron-based superconductors is the presence of a large incoherent peak at ~ 0.8 eV [11]. This incoherent peak is also observed in $\text{Tl}_{0.63}\text{K}_{0.37}\text{Fe}_{1.78}\text{Se}_2$, as shown in Fig. 4(a). While this broad peak is found to be dispersionless in k -space, it has a drastic temperature dependence between 35 K and 150 K, as shown in Fig. 4(a). The energy shift at this temperature range is about 100 meV, with much of the shift occurring below 100 K, as indicated in Fig. 4(b). This shift corresponds well with the metal-nonmetal crossover around 74 K observed in the resistivity of this material, which is shown in Fig. 4(c). Interestingly, the low-energy valence band below 0.3 eV is relatively insensitive to this crossover. This unusual dichotomy of energy shift between the high-energy incoherent feature and the low-energy dispersion could be consistent with the doped Mott insulator picture where quasiparticles emerge from a gapped incoherent background. These quasiparticles with renormalized effective mass and coherence residue form the observed low-energy dispersion and FS displayed in Figs. 4(d). Strong pairing observed on these FSs may be affected by the interaction happening beyond the vicinity of E_F [see Fig. 4(e)], even at an energy scale as large as the onsite Coulomb interactions.

The electronic structure of $\text{Tl}_{0.63}\text{K}_{0.37}\text{Fe}_{1.78}\text{Se}_2$ imposes severe constraints on the possible SC pairing mechanisms. The observation of nearly isotropic SC gap along two electron FS sheets near M is more consistent with scenarios for which the SC gap has the same sign on these two FSs. If they have opposite signs as for the d -wave gap would predict, nodes would likely emerge when the two bands hybridize. More significantly, superconductivity at high-temperature without holelike FS pocket strongly weakens the scenario of quasi-nesting-induced pairing of itinerant carriers. It is known that only the nested electron-hole FS pockets would lead to a logarithmic divergence in the particle-hole scattering channel, although interband scattering between two electronlike FS pockets as a key ingredient cannot be ruled out. On the other hand, it is possible that particle-hole scattering can utilize the “sinking” hole pocket which is not far from the Fermi energy [13]. In this case, a strong coupling with local pairing may be favored. In fact, good agreement with SC gap functions derived from a local picture were already found for other iron-pnictides [3, 12, 14–16].

In conclusion, our high-resolution ARPES measurements of the highly electron-doped $\text{Tl}_{0.63}\text{K}_{0.37}\text{Fe}_{1.78}\text{Se}_2$ superconductor reveal nearly isotropic superconducting gaps on the two nearly degenerated electron FS sheets at the M point. The SC gap with an amplitude of ~ 8.5 meV and closes above T_c , resulting in a pairing strength ($2\Delta/k_B T_c$ of ~ 7) twice stronger than the weak-coupling

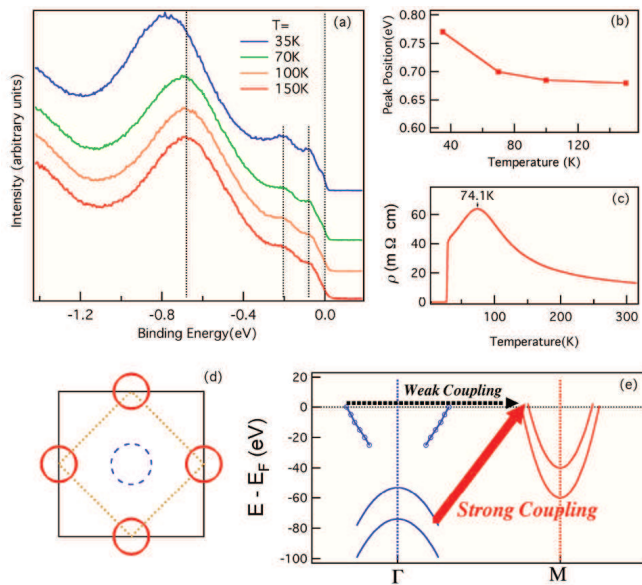


FIG. 4: (Colour on-line) (a) Temperature evolution of the wide energy range spectrum at the Γ point. (b) Temperature dependence of the peak position of the broad incoherent feature around 0.8 eV. (c) Temperature dependence of the resistivity of $\text{Tl}_{0.63}\text{K}_{0.37}\text{Fe}_{1.78}\text{Se}_2$, which indicates a metal-insulator transition at 74.1 K. (d) Schematic FS of $\text{Tl}_{0.63}\text{K}_{0.37}\text{Fe}_{1.78}\text{Se}_2$. (e) Schematic band structure of $\text{Tl}_{0.63}\text{K}_{0.37}\text{Fe}_{1.78}\text{Se}_2$.

BCS value. In addition, an unexpected electron Fermi surface with similar k_F and Δ is observed around the zone centre, along with a holelike band sinking ~ 50 meV below the Fermi energy. On the larger energy scale, the dispersionless incoherent peak at 0.7 - 0.8 eV shows a significant energy shift of ~ 100 meV when going through the metal-nonmetal crossover around 74 K, while the low-energy band structure is relatively unaffected.

We acknowledge W.-C. Jin, W.-D. Kong and H. Miao for technical assistance and X. Dai, Z. Fang, D.-H. Lee and D. J. Scalapino for useful discussions. This work is supported by Chinese Academy of Sciences (grant No. 2010Y1JB6), National Basic Research (973) Program of China (grants No. 2010CB923000, No. 2011CBA0010), and Nature Science Foundation of China (grants No. 10974175, No. 11004232, and No. 11050110422).

-
- [1] H. Ding, P. Richard, K. Nakayama, K. Sugawara, T. Arakane, Y. Sekiba, A. Takayama, S. Souma, T. Sato, T. Takahashi, Z. Wang, X. Dai, Z. Fang, G. F. Chen, J. L. Luo and N. L. Wang, *Europhys. Lett.* **83**, 47001 (2008).
- [2] L. Zhao, H.-Y. Liu, W.-T. Zhang, J.-Q. Meng, X.-W. Jia, G.-D. Liu, X.-Li Dong, G.-F. Chen, J.-L. Luo, N.-L. Wang, W. Lu, G.-L. Wang, Y. Zhou, Y. Zhu, X.-Y. Wang, Z.-Y. Xu, C.-T. Chen and X.-J. Zhou, *Chin. Phys. Lett.* **25**, 4402 (2008).
- [3] K. Nakayama, T. Sato, P. Richard, Y.-M. Xu, Y. Sekiba, S. Souma, G. F. Chen, J. L. Luo, N. L. Wang, H. Ding and T. Takahashi, *Europhys. Lett.* **85**, 67002 (2009).
- [4] K. Terashima, Y. Sekiba, J. H. Bowen, K. Nakayama, T. Kawahara, T. Sato, P. Richard, Y.-M. Xu, L. J. Li, G. H. Cao, Z.-A. Xu, H. Ding and T. Takahashi, *Proc. Natl. Acad. Sci. USA* **106**, 7330 (2009).
- [5] K. Nakayama, T. Sato, P. Richard, T. Kawahara, Y. Sekiba, T. Qian, G. F. Chen, J. L. Luo, N. L. Wang, H. Ding, and T. Takahashi, *Phys. Rev. Lett.* **105**, 197001 (2010).
- [6] T. Sato, K. Nakayama, Y. Sekiba, P. Richard, Y.-M. Xu, S. Souma, T. Takahashi, G. F. Chen, J. L. Luo, N. L. Wang and H. Ding, *Phys. Rev. Lett.* **103**, 047002 (2009).
- [7] Y. Sekiba, T. Sato, K. Nakayama, K. Terashima, P. Richard, J. H. Bowen, H. Ding, Y.-M. Xu, L. J. Li, G. H. Cao, Z.-A. Xu and T. Takahashi, *New J. Phys.* **11**, 025020 (2009).
- [8] Jiangang Guo, Shifeng Jin, Gang Wang, Shunchong Wang, Kaixing Zhu, Tingting Zhou, Meng He, and Xiaolong Chen, *Phys. Rev. B* **82**, 180520(R) (2010).
- [9] Minghu Fang, Hangdong Wang, Chiheng Dong, Zujuan Li, Chunmu Feng, Jian Chen and H.Q. Yuan, *arXiv:1012.5236v1* (2010).
- [10] Y. Zhang, L. X. Yang, M. Xu, Z. R. Ye, F. Chen, C. He, J. Jiang, B. P. Xie, J. J. Ying, X. F. Wang, X. H. Chen, J. P. Hu and D. L. Feng, *arXiv:1012.5980v1* (2010).
- [11] T. Qian, X.-P. Wang, W.-C. Jin, P. Zhang, P. Richard, G. Xu, X. Dai, Z. Fang, J.-G. Guo, X.-L. Chen and H. Ding, *arXiv:1012.6017v1* (2010).
- [12] Z.-H. Liu, P. Richard, K. Nakayama, G.-F. Chen, S. Dong, J.-B. He, D.-M. Wang, T.-L. Xia, K. Umezawa, T. Kawahara, S. Souma, T. Sato, T. Takahashi, T. Qian, Yaobo Huang, Nan Xu, Yingbo Shi, H. Ding and S.-C. Wang, *arXiv:1008.3265v1* (2010).
- [13] Fa Wang, Fan Yang, Miao Gao, Zhong-Yi Lu, Tao Xiang, and Dung-Hai Lee, *arXiv:1101.4390v1* (2011).
- [14] L. Wray, D. Qian, D. Hsieh, Y. Xia, L. Li, J. G. Checkelsky, A. Pasupathy, K. K. Gomes, C. V. Parker, A. V. Fedorov, G. F. Chen, J. L. Luo, A. Yazdani, N. P. Ong, N. L. Wang, and M. Z. Hasan, *Phys. Rev. B* **78**, 184508 (2008).
- [15] K. Nakayama, T. Sato, P. Richard, Y.-M. Xu, T. Kawahara, K. Umezawa, T. Qian, M. Neupane, G. F. Chen, H. Ding, and T. Takahashi, *Phys. Rev. B* **83**, 020501(R) (2011).
- [16] Y.-M. Xu, Y.-B. Huang, X.-Y. Cui, E. Razzoli, M. Radovic, M. Shi, G.-F. Chen, P. Zheng, N.-L. Wang, C.-L. Zhang, P-

C. Dai, J-P. Hu, Z.Wang and H. Ding, *Nature Phys.*,
DOI: 10.1038/NPHYS1879 (2011).